J. Fluid Mech. (1983), vol. 134, pp. 195–203
Printed in Great Britain

The final stage of decay of turbulence in stably stratified fluid

By H. J. PEARSON† AND P. F. LINDEN
Department of Applied Mathematics and Theoretical Physics, University of Cambridge, Silver Street, Cambridge CB3 9EW

(Received 18 March 1982 and in revised form 22 March 1983)

The linearized equations for the final stage of decay of turbulence in a stably stratified fluid are solved by three-dimensional Fourier transformation. For large Prandtl number, slowly decaying almost-horizontal modes of motion are identified. It is argued that these modes explain the experimental observation that patches of turbulence eventually settle out into a set of approximately horizontal striations. The most persistent vertical wavelength for a given geometry is determined and compared with quantitative observations from a set of experiments.

1. Introduction

The decay of turbulence in a stratified fluid is readily visualized by a shadowgraph (or schlieren) image of the flow. There are many such observations in the literature (see e.g. Pao 1973; Thorpe 1973; Lange 1974; Koop & Browand 1979; Lin & Pao 1979; Linden 1980), and they all show essentially similar things. Whatever the method of generating the turbulence, the initially chaotic pattern produced as the turbulence distorts the density stratification eventually settles out into a set of approximately horizontal striations. At this stage the motions are weak and the striations then remain without any apparent change in form until they eventually disappear. In this final stage of decay Lange (1974) found that density fluctuations decay faster than would occur by molecular diffusion alone. He argued that the density field must be driving slow viscously dominated motions. Streak photographs of aluminium particles, such as shown in figure 3 of Linden (1980), show that within this banded structure the motion is aligned with the striations.

The concept of the final stage of decay of turbulence in a homogeneous field was introduced by Batchelor & Townsend (1948*a*, *b*). In this last stage of motion after a turbulent event, internal Reynolds numbers are small and so the Navier–Stokes equations may be linearized, with quadratic inertia terms being ignored. They pointed out that this motion is not turbulent in the usual sense, as there is no cascade of energy from large to small scales and locally the flow is stable and laminar. However, the motion is the remnant from an initial truly turbulent motion and is disordered on a large scale.

In this paper we investigate the linearized equations of motion in the presence of a mean vertical density gradient. The introduction of stable stratification allows the transfer of fluid energy between kinetic and potential forms as well as its dissipation by viscosity. This is found to have interesting consequences for the type of motion that can occur. A very slowly decaying mode of motion is found giving nearly

† Present address: Smith Associates Consulting System Engineers Ltd, 45–47 High Street, Cobham, Surrey KT11 3DT.

horizontal cellular motions. It is argued that these modes describe the quasi-horizontal striations observed in decaying stratified turbulence. Simple experiments were performed to measure the vertical scale of these striations in a number of situations. Predictions of the vertical scales giving the slowest rates of decay were found to agree with the observed scales.

2. Linear equations and solution

We take rectangular Cartesian coordinates with the z-axis vertical and gravity given by $-g\hat{z}$, where $\hat{z}$ is a unit vector in the positive z-direction. We make the Boussinesq approximation, neglecting density differences except in the buoyancy term. We consider a linear mean density stratification given by $\bar{\rho}(z) = \rho_0(1-g^{-1}N^2z)$ with constant buoyancy frequency N. Here $\bar{\rho}(z)$ denotes the density averaged over the x- and y-directions for given z, and ρ_0 is a representative density, whilst ρ' will be used to denote the density perturbation from its mean value. The velocity components $\boldsymbol{u} = (u, v, w)$ are all small as we are linearizing about a state of rest. With p denoting the perturbation of pressure from its hydrostatic value the Navier–Stokes equations reduce to

$$\frac{\partial \boldsymbol{u}}{\partial t} = -\frac{1}{\rho_0}\nabla p - g\frac{\rho'}{\rho_0}\hat{z} + \nu\nabla^2\boldsymbol{u}, \tag{1}$$

where ν is the kinematic viscosity. For an incompressible fluid

$$\nabla\cdot\boldsymbol{u} = 0. \tag{2}$$

A fifth equation is provided by the linearized density-perturbation transport equation

$$\frac{\partial \rho'}{\partial t} - \frac{\rho_0}{g}wN^2 = \kappa\nabla^2\rho', \tag{3}$$

where κ is the diffusivity of the scalar (usually heat or a solute) providing the basic stratification.

We solve this set of equations by introducing three-dimensional Fourier transforms defined by

$$(u, v, w, p, \rho') = \iiint_{-\infty}^{\infty} \mathrm{e}^{\mathrm{i}\boldsymbol{k}\cdot\boldsymbol{r}}\,(\hat{u}(k), \hat{v}, \hat{w}, \hat{p}, \hat{\rho}')\,\mathrm{d}^3\boldsymbol{r}, \tag{4}$$

where $\boldsymbol{k} = (k_1, k_2, k_3)$ and $k_1^2+k_2^2+k_3^2 = k^2$. Substitution of (4) in (1)–(3) and then solving for $\hat{w}$ gives

$$\left(\frac{\partial}{\partial t}+\nu k^2\right)\left(\frac{\partial}{\partial t}+\kappa k^2\right)\hat{w} + N^2\left(\frac{k_1^2+k_2^2}{k^2}\right)\hat{w} = 0. \tag{5}$$

This equation has solutions

$$\hat{w}(\boldsymbol{k}, t) = A(\boldsymbol{k})\,\mathrm{e}^{\sigma_1 t} + B(\boldsymbol{k})\,\mathrm{e}^{\sigma_2 t}, \tag{6}$$

for arbitrary $A(\boldsymbol{k})$, $B(\boldsymbol{k})$, where

$$\sigma_{1,2} = -\tfrac{1}{2}(\nu+\kappa)\,k^2 \pm \tfrac{1}{2}[(\nu-\kappa)^2\,k^4 - 4\omega^2]^{\frac{1}{2}}, \tag{7}$$

and we have introduced a reduced frequency

$$\omega(\boldsymbol{k}) = N\left(\frac{k_1^2+k_2^2}{k}\right)^{\frac{1}{2}} = N\cos\theta,$$

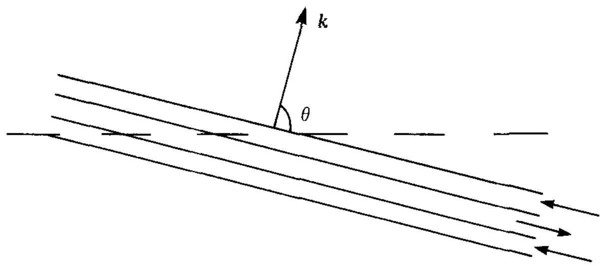

FIGURE 1. Schematic diagram of slowly decaying modes.

which is the frequency of an undamped (inviscid) internal gravity wave with wavevector $\boldsymbol{k}$, making an angle θ with the horizontal (see figure 1). Note that the real parts of σ_1 and σ_2 are always negative, so that in all cases $\hat{w}$ decreases with time. The result (6) may be compared with the result for an unstratified fluid

$$\hat{w}(\boldsymbol{k},t) = A(\boldsymbol{k})\,\mathrm{e}^{-\nu k^2 t}.$$

The perturbation density $\hat{\rho}'$ also satisfies (5), and the solution corresponding to (6) is just

$$\hat{\rho}'(\boldsymbol{k},t) = \frac{\rho_0}{g}N^2\left(\frac{A(\boldsymbol{k})}{\kappa k^2+\sigma_1}\mathrm{e}^{\sigma_1 t}+\frac{B(\boldsymbol{k})}{\kappa k^2+\sigma_2}\mathrm{e}^{\sigma_2 t}\right). \tag{8}$$

The horizontal velocity components satisfy the third-order equation

$$\left(\frac{\partial}{\partial t}+\nu k^2\right)\left(\frac{\partial}{\partial t}-\sigma_1\right)\left(\frac{\partial}{\partial t}-\sigma_2\right)\begin{Bmatrix}\hat{u}\\ \hat{v}\end{Bmatrix} = 0. \tag{9}$$

The third solution of this equation, different from those of (5), corresponds to purely horizontal motions decoupled from all buoyancy effects but with wavevector $\boldsymbol{k}$ that may have any orientation. These horizontal motions decay at the purely viscous rate $\exp[-\nu k^2 t]$.

3. Large-Prandtl-number solutions

If $Pr = \nu/\kappa \gg 1$, e.g. for water stratified with either common salt ($Pr = 800$) or heat ($Pr = 7.1$), then one might expect the purely diffusive decay of density perturbations to be much slower than the viscous damping of fluid motions. However, we show here that there are an interesting class of solutions in which the density and velocity fields are linked so that they both decay together at essentially the density diffusion rate.

Returning to (7) we see that there are two possibilities: (i) $(\nu-\kappa)k^2 < 2\omega$, giving complex roots so that the Fourier component is a damped but propagating internal wave; and (ii) $(\nu-\kappa)k^2 > 2\omega$, giving real and negative roots so each Fourier component just decays in time. In the first case there is a phase difference between the density and velocity fields but not in the second. The interesting limiting case is $(\nu-\kappa)k^2 \gg \omega$ where dissipation dominates buoyancy, either because the wavelength of the motion, $\lambda = 2\pi/k$, is small compared with the lengthscale $(\nu/N)^{\frac{1}{2}}$, or because the wave-vector is almost vertical ($k_3^2 \sim k^2$).

Expanding (7) in powers of $\omega/(\nu-\kappa)k^2$ to second order leads to

$$\sigma_1 \sim -\kappa k^2 - \frac{\omega^2}{(\nu-\kappa)k^2},$$

or

$$\sigma_1 = -\kappa k^2 - \frac{\omega^2}{\nu k^2}, \tag{10}$$

to lowest order in the inverse of the Prandtl number. Also

$$\sigma_2 = -\nu k^2 + \frac{\omega^2}{\nu k^2}. \tag{11}$$

The first root, σ_1, is of most interest as it is much smaller in magnitude than the viscous decay rate $-\nu k^2$ (note $\sigma_2 \approx -\nu k^2$): it consists of two parts, namely diffusive decay at the rate $-\kappa k^2$ and the new term $\omega^2/\nu k^2$. Note that the second part of $-\sigma_1$ is an increasing function of N but, perhaps unexpectedly, a decreasing function of viscosity and wavenumber. This solution represents a slow creeping motion where buoyancy forces are balanced by viscous forces. Increasing the viscous forces (νk^2) decreases the rate at which potential energy is released from the perturbation density field. The solution (10) can be obtained directly from (5) by making a zero-Reynolds-number approximation, that is to say neglecting the (inertial) time-derivative term in (1), which leads to

$$\left(\frac{\partial}{\partial t} + \kappa k^2 + \frac{\omega^2}{\nu k^2}\right)\hat{w} = 0.$$

For any given wavenumber k the smallest value of $\omega^2/\nu k^2$ will occur for nearly vertical wave-vectors. As time increases, the flow field will be dominated more and more by almost-horizontal motion in flat cells of far greater horizontal than vertical extent. (As is, in fact, observed in experiments as described in §5.) The horizontal velocities are much larger than the vertical velocities in such a motion. This can be seen by computing, say, $\hat{u}$ assuming $\hat{w}$ has time dependence $\exp[\sigma_1 t]$. Then using (1), (2) and (8) and assuming $k_3 \sim k$, $k_1 \sim k_2$ and putting $\kappa = 0$ for simplicity

$$\frac{\hat{u}}{\hat{\omega}} \sim \left(\frac{\nu k^2}{N}\right)^2 \left(\frac{k}{k_1}\right)^2,$$

which will be large for $k_1 \ll k$ even if $N \sim \nu k^2$.

It can be seen that similar results arise for $Pr \ll 1$, but with ν and κ reversed in (10), (11) and most subsequent results. However, a difference in this case is that the purely viscous terms in (9), which are decoupled from buoyancy effects, now give the slowest-decaying part of the solution.

4. Most slowly decaying mode

The wavenumber of the most slowly decaying mode is determined from (10), and for constant wave-vector angle θ is given by

$$k^4 = \frac{N^2}{\nu\kappa}\cos^2\theta, \tag{12}$$

whence

$$\sigma_1 = -2\left(\frac{\kappa}{\nu}\right)^{\frac{1}{2}} N\cos\theta, \tag{13}$$

or in terms of the wavelength of the disturbance

$$\lambda = 2\pi\left(\frac{\nu\kappa}{N^2\cos^2\theta}\right)^{\frac{1}{4}}. \tag{14}$$

For modes with this wavelength the two terms in (10) are equal and the decay of the density field is due equally to convection and molecular diffusion. Also note that we may rewrite (12) as

$$\frac{\omega}{\nu k^2} = \left(\frac{\kappa}{\nu}\right)^{\frac{1}{2}} = Pr^{-\frac{1}{2}} \ll 1,$$

and so (12) is consistent, for large Prandtl number, with the expansion leading to (10).

Equation (13) suggests that $|\sigma_1|$ may be made infinitesimally small by taking θ arbitrarily close to $\frac{1}{2}\pi$. However, this corresponds to disturbances of infinite horizontal extent, which is not compatible with either a finite container or the generation of finite patches of turbulence in an unbounded fluid. Therefore a realistic estimate of the minimum decay rate requires a lower bound to be put on the horizontal wavenumbers of the disturbance, say

$$k_1^2 + k_2^2 \geqslant l^2. \tag{15}$$

(The interaction of these quasi-horizontal modes with solid boundaries is analysed in Pearson (1981).)

It is shown in the appendix that the minimum of value of $|\sigma_1|$ subject to (15) will occur at equality

$$k_1^2 + k_2^2 = l^2,$$

and is given by

$$k_{\min} = \left(\frac{2N^2l^2}{\nu\kappa}\right)^{\frac{1}{6}}, \tag{16}$$

so that

$$(-\sigma_1)_{\min} = 1.89Pr^{-\frac{2}{3}}(\nu N^2 l^2)^{\frac{1}{3}}.$$

Note that the vertical wavelength of the most persistent mode is only weakly dependent on the Prandtl number (one-sixth power), the stratification and the maximum horizontal scale.

Recently, Ivey & Corcos (1982) have obtained the same result as (16) (see their equation (14)) for the horizontal decay of layers generated by the oscillation of a vertical grid in a stably stratified fluid.

The scaling (14) is the same as that for the thickness of the buoyancy layer that can occur on a solid boundary, at an angle θ to the horizontal, in a stable density gradient (see Turner 1973, pp. 243–245). This boundary-layer flow is induced by imposing either a constant density difference (Prandtl 1952, p. 422) or no normal density flux (Phillips 1970; Wunsch 1970) at the sloping wall. However, the slowly decaying modes described here do not represent a stack of buoyancy layers one on top of another. Although the scalings are the same, for dimensional reasons, they have different underlying physical mechanisms. Our quasi-horizontal motions are driven by the potential energy of the system and involve a partial 'unmixing' or reduction of this potential energy. On the other hand buoyancy layers are driven by molecular diffusion and involve a 'mixing-up' of the system.

5. The experiments and comparison of results

In the present experiments the vertical scale of the quasi-horizontal striations observed during the final stage of decay was measured from a shadowgraph image in a number of different situations. Both salt (Pr = 800) and heat (Pr = 7.1) were used

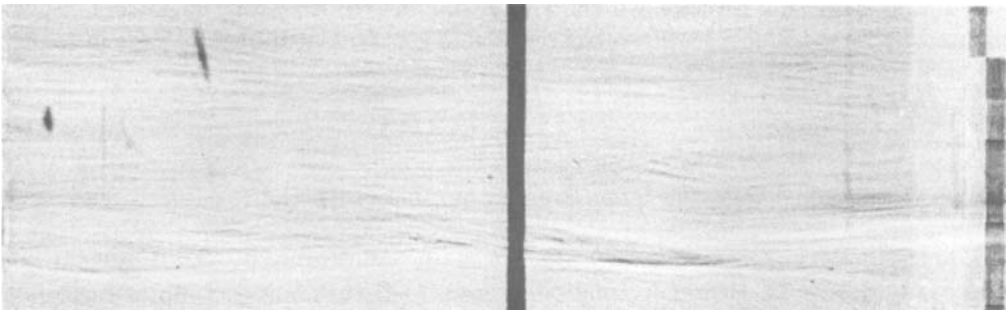

1 cm

FIGURE 2. Shadowgraph of slowly decaying quasi-horizontal motions. This photograph was taken approximately 2 min after a grid of horizontal bars had been passed vertically through the fluid. In this case $N = 1.23\ \mathrm{s}^{-1}$.

to produce stratified water columns, and these were stirred in a variety of ways. Three different tank sizes were used measuring respectively 25.4×25.4 cm, 58.4×58.4 cm and 10.8×45.6 cm in cross-section. In the first two of these tanks, the turbulence was generated by allowing grids composed of square or round bars (1 cm bar width with 5 cm mesh in the small tank and 2.3 cm bar width with 11.5 cm mesh in the large tank) to fall vertically through the fluid in the manner described by Linden (1980). In the other tank the fluid was stirred by 'whisking' it with a vertical rod. The density gradient was measured before and after each run and the value of the buoyancy frequency N (s^{-1}) was computed from the final value, as that was representative of the density field when the striations were present.

Quantitative information of the size of the striations was obtained by measuring their scale from still photographs of the shadowgraph image. An example of the quasi-horizontal modes obtained by passing a grid vertically through the fluid with an initially constant density gradient is shown on figure 2. The vertical scale was determined by counting the number of striations (usually 10–40) over a vertical span of 5–10 cm, and so each value represents an average size.

In a number of the experiments in the rectangular tank, measurements of the thickness of the striations were obtained simultaneously from shadowgraphs through the front and the sides of the tank. No differences between the data were observed, indicating that the finite pathlength of light through the tank does not bias the estimation of the vertical scale of the striations. Since the deflections of light in a shadowgraph system are caused by changes in refractive index gradient, it is necessary to double the vertical scale obtained in this way in order to determine the mean vertical wavelength λ of the density variations.

The results are summarized in figure 3, which shows λ non-dimensionalized by D, the length of the diagonal of the tank. If the disturbance scale is limited by the maximum scale of the experimental tank then (16) implies that

$$\frac{\lambda}{D} = (2\pi)^{\frac{2}{3}}\left(\frac{\nu\kappa}{2N^2D^4}\right)^{\frac{1}{6}}. \tag{17}$$

In figure 3 the straight line represents the theoretical relationship (17). There is considerable scatter in the experimental data, but (17) seems to provide a good estimate of the vertical scale of the striations.

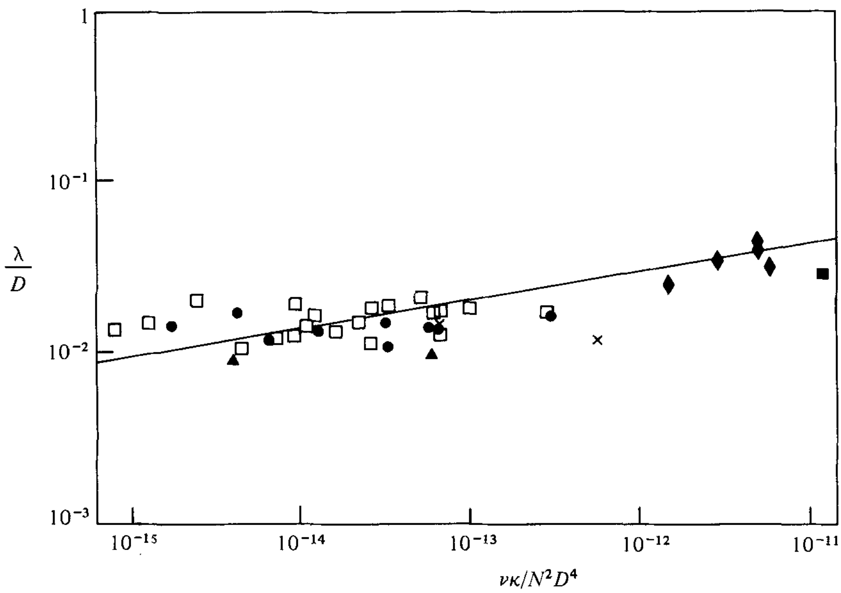

FIGURE 3. The mean vertical spacing λ of the striations plotted against $\nu\kappa/N^2D^4$ on log–log scales. Salt stratification: □, square-bar grid, ●, round-bar grid, $D = 35.9$ cm; ▲, square-bar grid, $D = 82.6$ cm; ×, square-bar grid, $D = 35.9$ with initially linear gradient. Heat stratification: ■, square-bar grid, $D = 35.9$, ◆, arbitrary stirring, $D = 46.8$ cm. The straight line is the predicted relationship (17).

Immediately after the passage of the grid the most-energetic wavenumber of the turbulent field probably scales on the mesh size of the grid and not the tank dimension. However, during the initial nonlinear phase of motion, stratification acts to make the flow more anisotropic, decreasing vertical scales and increasing horizontal scales. This can be thought of as the collapse of mixed or partially mixed regions of fluid as they spread horizontally at a height corresponding to their density. An example of this process is seen in the case of the cross-stream collapse of the wake of a body in a horizontal flow (Lin & Pao 1979).

As long as sufficient energy is put into the turbulence by the grid, this increase of maximum horizontal scale continues until limited by the walls of the tank.

6. Conclusions

In this paper we have shown that the final stage of decay of a turbulent mixing event in a stable density gradient is described by solutions of the linearized equations of motion. We find that for large Prandtl number the most persistent motions are almost horizontal and have a short vertical wavelength. The vertical velocity and density fluctuations associated with these modes are in phase, and they decay as a result of advection and molecular diffusion. The motions are driven by potential energy stored in small (vertical) scale fluctuations of the density gradient, which have been previously produced by the turbulent event. They provide the mechanism by which the isopycnals eventually become horizontal and all motion ceases.

Since these modes are driven by the density field and are opposed by viscous stresses, an increase in the fluid viscosity slows down the release of potential energy. However, the motion will persist until all the potential energy is released and so we have the (at first sight paradoxical) result noted in §4 that the decay rate decreases as the viscosity increases. The decay rate as given by (10) is faster than that obtained by molecular diffusion alone, as had been noted by Lange (1974) in a discussion of his experimental results.

For an imposed horizontal lengthscale D, the vertical wavelength λ/D of the most-persistent mode is predicted to scale on $(\nu\kappa/N^2D^4)^{\frac{1}{6}}$. Experimental measurements of λ/D, under conditions where the turbulence is fairly homogeneous in the horizontal and where D is taken to be the size of the container, support this prediction. However, the dependence of λ on all the parameters is weak and it has not been possible to make a test of the scaling law which rules out other possibilities. In natural situations, when the turbulence is produced by, say, the collapse of a mixed region or by the breaking of an internal wave, the horizontal scale of the turbulent patch will depend upon the early energetic stages of the motion.

Small-scale density structures have often been found in the stably stratified interiors of the oceans. In some circumstances there appears to be no velocity signal associated with density perturbation and it has been concluded that the density field marks a turbulent event from which the velocity field has decayed (since the Prandtl number is greater than unity). This kind of structure has been called 'fossil turbulence' by oceanographers. The work described here shows that there is a velocity perturbation associated with this density field, at least until all the isopycnals are horizontal.

H.J.P. was supported by a Natural Environment Research Council studentship while undertaking this research. He would like to thank Dr J. C. R. Hunt, for suggesting and supervising the theoretical part of this work, and Dr J. S. Turner, for drawing his attention to the similarity between the scaling (14) and that for buoyancy layers. The paper was completed while H.J.P. was a visitor in the Environmental Engineering Science department of the California Institute of Technology.

Appendix

We need to minimize

$$(-\sigma_1) = \kappa k^2 + N^2\frac{(k_1^2+k_2^2)}{\nu k^4}, \tag{A 1}$$

subject to the condition

$$k_1^2+k_2^2 \leqslant l^2. \tag{A 2}$$

Suppose $k_1^2+k_2^2 = c^2$, a constant, then (A 1) becomes

$$(-\sigma_1) = \kappa(c^2+k_3^2)+\frac{N^2c^2}{\nu(c^2+k_3^2)^2}. \tag{A 3}$$

Differentiating (A 1) with respect to k_3, we find that the minimum value is given by

$$k^6 = (c^2+k_3^2)^3 = \frac{2N^2c^3}{\nu\kappa},$$

which on substituting into (A 3) gives

$$(-\sigma_1) = 3\left(\frac{k^2N^2c^2}{2\nu}\right)^{\frac{1}{3}},$$

which is a monotonically increasing function of c. Therefore the minimum value of (A 1) subject to (A 2) is for the minimum value of c, i.e. $k_1^2+k_2^2 = l^2$. Thus

$$k_{\min} = \left(\frac{2N^2l^2}{\nu\kappa}\right)^{\frac{1}{6}},$$

$$(-\sigma_1) = 1.89Pr^{-\frac{2}{3}}(\nu N^2 l^2)^{\frac{1}{3}}.$$

REFERENCES

BATCHELOR, G. K. & TOWNSEND, A. A. 1948*a* Decay of isotropic turbulence in the initial period. *Proc. R. Soc. Lond.* **A193**, 539–558.

BATCHELOR, G. K. & TOWNSEND, A. A. 1948*b* Decay of isotropic turbulence in the final period. *Proc. R. Soc. Lond.* **A194**, 527–543.

IVEY, G. N. & CORCOS, G. M. 1982 Boundary mixing in a stratified fluid. *J. Fluid Mech.* **121**, 1–26.

KOOP, C. G. & BROWAND, F. K. 1979 Instability and turbulence in a stratified fluid with shear. *J. Fluid Mech.* **93**, 135–159.

LANGE, R. E. 1974 Decay of turbulence in stratified salt water. Ph.D. thesis, University of California at San Diego.

LIN, J. T. & PAO, Y. H. 1979 Wakes in stratified fluids. *Ann. Rev. Fluid Mech.* **11**, 317–338.

LINDEN, P. F. 1980 Mixing across density interfaces produced by grid turbulence. *J. Fluid Mech.* **100**, 691–709.

PAO, Y.-H. 1973 Measurements of internal waves and turbulence in two-dimensional stratified shear flows. *Boundary-Layer Met.* **5**, 177–193.

PEARSON, H. J. 1981 Disturbances and displacements in stratified fluids. Ph.D. thesis, University of Cambridge.

PHILLIPS, O. M. 1970 On flows induced by diffusion in a stably stratified fluid. *Deep-Sea Res.* **17**, 435–443.

PRANDTL, L. 1952 *Essentials of Fluid Dynamics*. Blackie.

THORPE, S. A. 1973 Turbulence in stably stratified fluids: a review of laboratory experiments. *Boundary-Layer Met.* **5**, 95–119.

TURNER, J. S. 1973 *Buoyancy Effects in Fluids*. Cambridge University Press.

WUNSCH, C. 1970 On oceanic boundary mixing. *Deep-Sea Res.* **17**, 293–301.